Structural relaxation in a viscous liquid studied by quasielastic nuclear forward scattering

I. Sergueev,[1,2] H. Franz,[3] T. Asthalter,[4] W. Petry,[1] U. van Bürck,[1] and G. V. Smirnov[5]
[1]*Technische Universität München, Physik Department E13, D-85747 Garching, Germany*
[2]*European Synchrotron Radiation Facility, BP 220, F-38043, Grenoble, France*
[3]*Hamburger Synchrotronstrahlungslabor, Deutsches Elektronen Synchrotron, D-22603 Hamburg, Germany*
[4]*Universität Stuttgart, Institut für Physikalische Chemie, D-70569 Stuttgart, Germany*
[5]*Russian Research Center "Kurchatov Institute," 123182 Moscow, Russia*
(Received 21 June 2002; published 27 November 2002)

Quasielastic nuclear forward scattering (QNFS) of synchrotron radiation is employed as a probe of slow glass dynamics, in particular for the determination of the stretching parameter β in the Kohlrausch-Williams-Watts relaxation function. The influence of this type of relaxation on multiple scattering is investigated in detail, and experimental results on the dynamics of the molecular glass former ferrocene/dibutylphthalate in the undercooled viscous state are presented. We observe a temperature independent stretching parameter of 0.47(2). Fitting the high temperature breakdown of the Lamb-Mössbauer factor with a square root dependence we obtain a mode-coupling critical temperature of $T_c = 202$ K.

DOI: 10.1103/PhysRevB.66.184210 PACS number(s): 61.10.Dp, 66.30.−h, 76.80.+y

I. INTRODUCTION

Since the first publications on mode coupling theory (MCT) applied to the critical freezing of viscous liquids considerable progress has been achieved in understanding the microscopic origin of the liquid-to-glass transition. Initiated by scaling predictions of MCT,[1] the microscopic dynamics of viscous liquids has been studied in great detail (see, e.g., Ref. 2, and references therein). One of the generally accepted facts is that the final decay of the density-density correlation function (relaxation function) $F(t)$, which describes the so called α-relaxation, is stretched when compared to a simple exponential decay,[3] however its precise shape is a matter of actual debate. A simple but common description of this relaxation regime in the time domain is based on the Kohlrausch stretched exponential[4,5]

$$F(t) = f_q \exp[-(t/t_r)^{\beta}]. \tag{1}$$

Here f_q is the nonergodicity parameter describing the decay of the correlations due to any process faster than the α-relaxation, i.e., phonon dynamics and fast local relaxations (the cage or MCT β process), β is a stretching parameter with $0<\beta<1$ quantifying the deviation of $F(t)$ from the behavior of a simple Debye relaxator ($\beta=1$), and t_r is the characteristic relaxation time. In the frequency domain spectra are usually described by the empirical Havriliak-Negami function[6] or simplified versions, such as the Cole-Cole[7] or Cole-Davidson function[8] both very similar to the Fourier transform of Eq. (1).

Experimentally this form of the relaxation function is found in quasielastic neutron scattering, light scattering, or dielectric spectroscopy measurements for a wide range of glass-forming systems. Concerning the microscopic origin of the stretching there are two pictures discussed in literature: it may either be due to a spatial distribution of simple exponential relaxations (heterogeneous picture)[9] or, alternatively, to a correlated relaxation of a cage formed by the neighborhood (homogeneous picture)[10] which leads to an inherently nonexponential relaxation of each individual unit.

It should be noted that also MCT (Refs. 1,11) predicts the existence of a stretched exponential relaxation. The Kohlrausch law can be derived as the high-wave-vector limit of the MCT equations.[3]

Resonant nuclear forward scattering (NFS) of synchrotron radiation is a relatively new scattering technique[12] that reveals directly in the time domain the relaxational dynamics of the resonant Mössbauer isotope. NFS is the spatially coherent scattering variant of classical Mössbauer spectroscopy, which has also been used to study collective motions in glass-forming liquids (for a review and recent results see, e.g., Refs. 13,14). NFS has been demonstrated both theoretically[15] and experimentally[16] to yield information about the self-part of the density-density correlation function in a time window of a few nanoseconds up to microseconds at atomic length scales. This length scale is determined by the fixed wave-vector $q = 7.3$ Å^{-1} for experiments with ^{57}Fe. This time window extends the range of dynamics covered by neutron scattering techniques (picoseconds up to a few nanoseconds).[17] Moreover, it provides a link to data from light scattering techniques or dielectric-loss spectroscopy that cover a similar time window but at much larger or even ill-defined length scales.[2] This is exactly the time range where the critical glass dynamics predicted by MCT is found in most low-molecular-weight glass formers.

Thus NFS opens the way to study the structural (α-) relaxation around and in particular below the MCT crossover temperature T_c. Neutron experiments in contrast hardly ever supply data near T_c.[18] However, NFS requires a resonant isotope in the sample, for practical purposes a decent amount of iron in the sample. This certainly restricts the selection of suitable systems.

In this paper, we present results using NFS on a molecular glass former that allow us to determine unambiguously the Kohlrausch stretching parameter for relatively large wavevectors, i.e., on sub-Å length scales. Also we elucidate in general the rather complicated influence of a particular

nonexponential relaxation (Kohlrausch relaxation) on nuclear resonant multiple scattering.

The paper is organized as follows. After presenting the theoretical basis of nuclear resonant scattering in the presence of Kohlrausch relaxation, we briefly describe the experiment and our method of data evaluation. We then discuss our results in the light of the theoretical predictions and related experimental results.

II. THEORY

A. General

The theory of the influence of relaxation on scattering and absorption cross-sections in kinematical approximation goes back to the basic papers of Singwi and Sjölander covering both quasielastic neutron scattering[19] and quasielastic Mössbauer spectroscopy.[20] Whereas these first papers deal with energy resolved spectroscopy, experimental progress allows meanwhile to observe the relaxation directly in the time domain, i.e., by neutron spin echo[21] and nuclear resonant scattering (NRS).[22] The general theory of the influence of slow relaxation on the coherent quasielastic nuclear forward scattering of synchrotron radiation (QNFS) was derived in Refs. 15,23.

The time-dependent electric field amplitude $E(\tau)$ of radiation transmitted through a target with a single transition (no hyperfine interaction) in the forward direction can be represented as Fourier transformation of the response function of the target[24]

$$E(\tau)=\frac{A}{\tau_0}\int_{-\infty}^{\infty}\frac{d\omega}{2\pi}e^{-i\omega\tau}e^{-\xi_0\varphi(\omega)}, \tag{2}$$

where $\tau=t/\tau_0$ is the time scaled by the lifetime of the excited nuclear level τ_0 ($\tau_0=141.1$ ns for ^{57}Fe), ω is the frequency scaled by the inverse lifetime, $A=\sqrt{I/\Delta\omega}\exp(-\mu_e z/2)$ is the amplitude of the incident radiation multiplied by the electronic absorption in the target, $\xi=f_{LM}\xi_0=f_{LM}\sigma_0 n\eta z/4$ is the effective thickness parameter of the target. It is proportional to the resonance cross section σ_0, the Fe number density n, ^{57}Fe enrichment η, thickness of the target z and the Lamb-Mössbauer-factor (or recoil-free fraction) f_{LM}. The universal resonance function $\varphi(\omega)$ depends on the relaxation function $F_s(t)$ as follows:[15]

$$\varphi(\omega)=\int_0^{\infty}d\tilde{\tau}\,e^{i\omega\tilde{\tau}-\tilde{\tau}/2}F_s(\tilde{\tau}). \tag{3}$$

Note that $F_s(t)$ here is the full van Hove self-correlation function taking into account both fast and slow atomic motion. This is in contrast to some older papers where fast and slow motion were divided rather artificially.

Combining Eq. (2) and Eq. (3) in time domain, as is done in the Appendix, we can write the intensity of the delayed signal as [see Eq. (A7)]

$$I(\tau)=I_{\rm kin}(\tau)R^2(\tau), \tag{4}$$

$$I_{\rm kin}(\tau)=\left(\frac{A}{\tau_0}\right)^2\xi_0^2e^{-\tau}F_s^2(\tau). \tag{5}$$

This set of equations describes the scattered intensity in general. The factor $R(\tau)$ in Eq. (4) results from multiple scattering of the γ quantum by the nuclear ensemble. Due to the relatively large resonance cross section of the nuclear scattering, multiple scattering turns out to be important for many experiments.

In absence of relaxation [$F_s(t)=$const] the analytical expression

$$R(\tau)=\frac{J_1(2\sqrt{\xi\tau})}{\sqrt{\xi\tau}} \tag{6}$$

was derived[24] (see also overview Ref. 25), where $J_1(x)$ is the Bessel function of first kind and first order. The function $R^2(\tau)$ shows oscillations called dynamical beats (DB) with minima at $\xi\tau=3.7,\ 12.3,\ \ldots$, defined by the roots of the Bessel function. The DB modulation originates from the continuous energy exchange between the radiation field and the nuclear oscillator system by multiple scattering.[25,26] Note that the apparent beat periods increase with time and decrease with optical thickness in a characteristic way. This simple relation between quasiperiodicity in the dynamical beating and effective thickness is an important tool to extract information from experimental data.

When the value of $\xi\tau$ is relatively small, mostly the interaction of the primary radiation with the nuclei is essential and the factor $R(\tau)$ may be approximated by $\exp(-\xi\tau/2)$.[27] This approximation holds in the time region near zero time and its validity extends to larger time with decreasing effective thickness.

B. Stretched exponential relaxation

In this chapter we will focus on relaxations described by the Kohlrausch self-correlation function

$$F_s(\tau)=f_q\exp[-(\tau/\tau_r)^{\beta}], \tag{7}$$

where $\tau_r=t_r/\tau_0$ is the rescaled relaxation time. In this context f_q is equal to the Lamb-Mössbauer factor $f_{\rm LM}$ describing relaxations faster than the accessible time window. The separation of fast and slow relaxation is a purely technical issue which results from the finite width of the exciting synchrotron pulse and the performance of the detectors.[28] In the case of glass dynamics at least both phonon vibrations and MCT β-relaxation are included in $f_{\rm LM}$. In a more stringent treatment of the short time behavior ($t\ll 1$ ns) $f_{\rm LM}$ must be replaced by a time-dependent term.

In kinematical approximation the intensity for this type of relaxation is given by Eq. (5). The time dependence of the intensity is shown in Fig. 1 for different β. The deviation of β from one appears as a bending-up of the correlation function and accordingly of the intensity on a logarithmic scale. The determination of β is most reliable in the time range where the intensity curve shows the strongest curvature. This occurs at very early times where the decay is much faster than natural. The observation in this range, however, is dif-

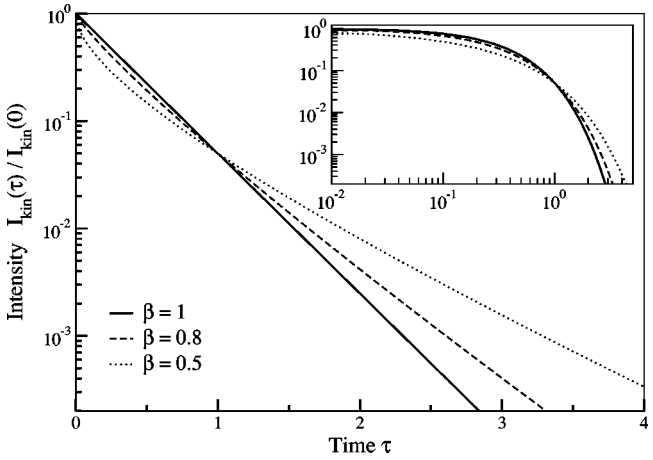

FIG. 1. Kinematical approximation of the delayed intensity for different β and $\tau_r = 1$ in lin/log and log/log (inset) scales.

ficult. In order to extract the non-exponential behavior in the kinematical approximation one has to observe the signal at least over two decades of time[11] (see inset in Fig. 1).

When $\xi\tau$ is relatively large (large effective thickness or long observation times) multiple scattering becomes important and the dynamical beat structure appears in the accessible time window. Fast relaxations described by f_{LM} just stretch the DB structure in time. It is important to notice that the coefficient of stretching is the same for the entire time region and equal to f_{LM}. Phenomenologically one can say that only a fraction of the nuclei inside the target takes part in the process of scattering.

For the simplest case of slow relaxation, i.e., free diffusion with a simple exponential self-correlation function, it was shown that the multiple scattering term $R(\tau)$ is not modified. The self-correlation function enters only as an additional exponential factor in Eq. (4).[15] Any other self-correlation function influences the multiple scattering term $R(\tau)$. In Fig. 2 we show the forward scattered intensity $I(\tau)$ under the influence of a stretched exponential relaxation for different values of β and τ_r. The effective thickness parameter ξ is taken to be 10. One can see that for $\beta = 1$ the positions of the DB minima are identical for any value of the relaxation time τ_r. The positions depend only on ξ. With decreasing β the DB minima shift to larger times. The same effect is observed for decreasing τ_r for a given $\beta < 1$. In other words, the intensity curve is stretched over the time axis like in the case of decreasing ξ, but now the stretching coefficient depends on time. The shifts of the first, second and third DB minima, normalized to the value of the corresponding minimum for the static case, are shown in Fig. 3 as a function of relaxation rate $\lambda_r = 1/\tau_r$. One can see that all curves can be separated into three parts: λ_r close to zero (long relaxation time) where a root dependence is observed, a region of large λ_r where the curves drastically rise and a transition region. One can show analytically (see appendix) that for relaxation times much larger than the nuclear life time τ_0 the relative shift of the ith DB minimum is

$$\Delta_i = A_i \lambda_r^{\beta}, \tag{8}$$

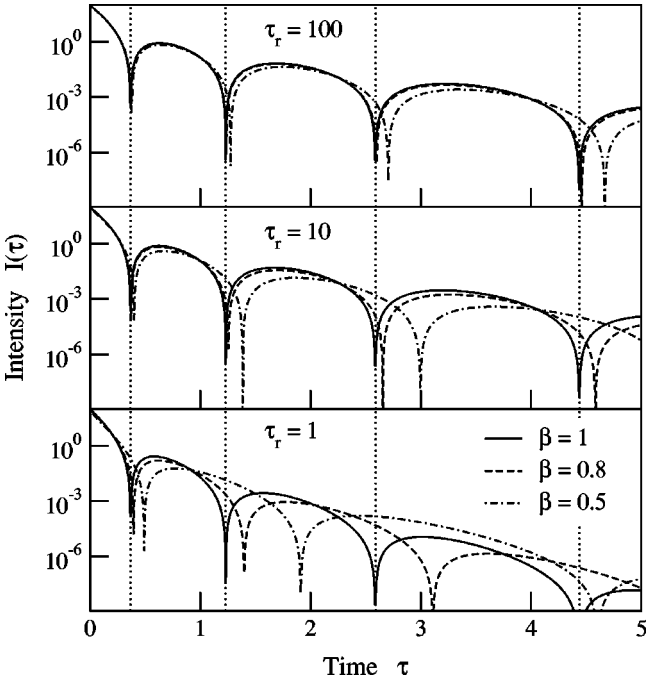

FIG. 2. Delayed intensity taking into account multiple scattering for different β and τ_r. The effective thickness parameter was chosen as $\xi = 10$.

where A_i is a coefficient independent of λ_r. For the case of $\beta = 0.5$ we obtain a square root dependence. The result is that even for very long relaxation times τ_r the shift of the DB minima is quite appreciable due to the behavior of the square root function near zero. By contrast the relative shifts of the DB minima as a function of f_{LM} (e.g., no slow relaxation) coincide, as shown in the inset of Fig. 3 and show a linear dependence for large f_{LM}.

To understand the behavior of the DB structure in detail, it is useful to consider also the frequency domain. In the gen-

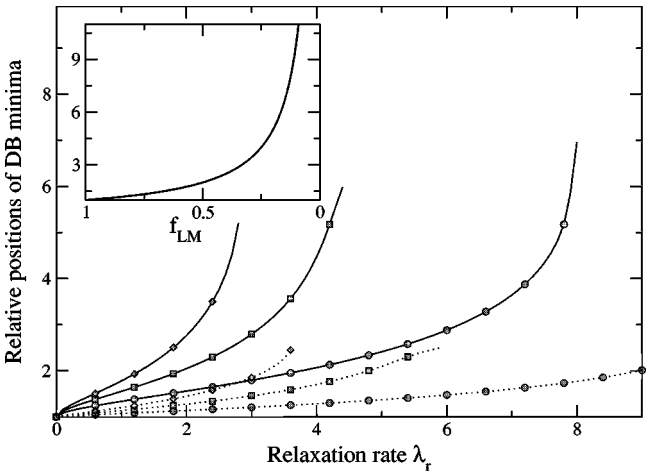

FIG. 3. Relative positions of the DB minima as a function of relaxation rate. Circles: first minimum, squares: second minimum, diamonds: third minimum, solid line: $\beta = 0.5$, dotted line: $\beta = 0.8$. In the inset we show relative positions of the DB minima (all three curves coincide) as a function of f_{LM}, i.e., the case of fast relaxation.

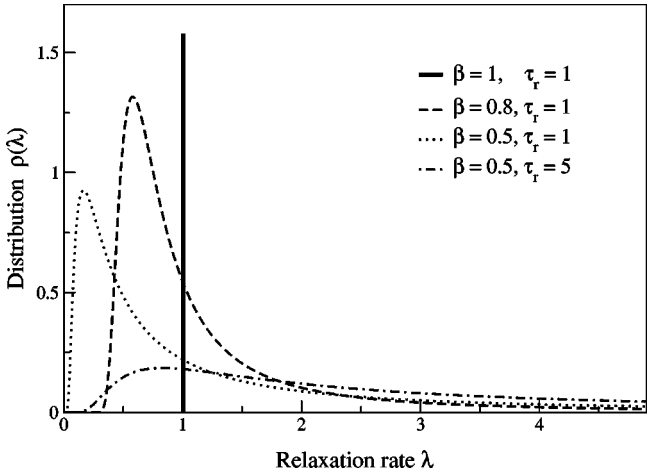

FIG. 4. Distribution of exponential decays over relaxation rate for a Kohlrausch self-correlation function.

eral theory diffusion manifests itself as an averaging over Doppler shifts of the resonance energy.[15] Accordingly we present the Kohlrausch function as a distribution of exponential decays over relaxation rates

$$F_s(\tau)=\int_0^\infty d\lambda e^{-\lambda\tau}\rho(\lambda). \tag{9}$$

The function $\rho(\lambda)$ is shown in Fig. 4 for different β and τ_r.

For $\beta=1$ the distribution is a delta function. The rate of dephasing between the radiation field and the nuclear ensemble is independent of time and identical for each nucleus.

For $\beta<1$ the distribution has a cutoff at the low-frequency side and a very long tail at high frequencies. One can interpret this distribution phenomenologically as a distribution of nuclei in the target, each of which has an exponential self-correlation function with a certain frequency, depending on position or/and time. It accounts for both the homogeneous and the heterogeneous picture of the stretched relaxation. In the first case the stretched relaxation is interpreted as the envelope of instantaneous exponential relaxators with a time-dependent relaxation rate. In the second case we have a spatial distribution of exponential relaxators, each of which has its individual now time-independent relaxation rate.

We can interpret the shifts of the DB minima as shown in Fig. 3 as due to an apparent decrease of the effective thickness of the target. γ quanta reemitted from nuclei with large λ run out of phase rather soon and are effectively lost for multiple forward scattering at later times. Thus with increasing time less and less nuclei participate in multiple forward scattering, and therefore the DB minima become more and more shifted to later times. This picture, which is used here for a continuous distribution of exponential decays, has been introduced originally in the study of jump diffusion for a discrete set of exponential decays with different weights and relaxation rates.[23,29]

The high sensitivity of the positions of the different DB minima to the Kohlrausch parameter β, as displayed in Figs. 2 and 3, is a key feature of multiple nuclear scattering under relaxation conditions. For sufficiently thick targets it will allow one to determine β and τ_r as a function of temperature with high precision. This holds until for small τ_r the NFS signal decays too fast so that the late evolution of the DB structure cannot be observed any longer.

III. THE EXPERIMENT

As a model substance we have chosen the molecular glass former 95% dibutylphthalate/5% ferrocene which has been the subject of a previous QNFS study in a time window up to 176 ns.[16] The procedure to obtain samples enriched in ^{57}Fe in high yield is described in Ref. 30.

First studies were carried out at the low-energy section of the PETRA undulator beamline at Hasylab, PETRA1.[31] The filling modes were 8 bunch and 16 bunch, resulting in time windows of 960 and 480 ns, respectively. An indirectly water-cooled diamond(111) high-heat load monochromator and a sapphire backscattering setup as high resolution monochromator[32] were used. Further QNFS experiments were carried out at the beamlines ID18 and ID22N at the European Synchrotron Radiation Facility.[33,34] A Si(111) high-heat load monochromator with He gas (ID18) or LN_2 cooling (ID22N) and a 6 meV four-bounce high-resolution monochromator serve to increase the ratio of incoming resonant to nonresonant x-ray quanta and thus reduce the load of the detectors. To obtain QNFS spectra within a long time window, single bunch mode with a time window of 2800 ns and hybrid bunch mode with a time window of 930 ns were used.

The sample temperature was varied between 40 and 202 K, using a closed-cycle helium cryostat having a stability better than ± 0.5 K. The reproducibility of the true sample temperature was estimated to 1 K. The sample was mounted in copper holders sealed with Kapton windows.

IV. DATA TREATMENT

Equation (4) describes the delayed intensity in the case of a single excited level of the nucleus. In the case of ferrocene the quadrupole splitting of the excited level changes the delayed intensity as follows (under the assumption that the levels are well separated)

$$I'_{\mathrm{del}}(\tau)=I_{\mathrm{del}}(\tau)4\cos^2[\Omega(\tau-a)/2], \tag{10}$$

where Ω is the value of the quadrupole splitting, a is a phase shift due to the mutual influence of the quadrupole lines[27] and $I_{\mathrm{del}}(\tau)$ is equal to $I(\tau)$ from Eq. (4) with ξ replaced by $0.5\,\xi$ because of the splitting into two lines. In accordance with the results of Ref. 35 we assume here that rotational relaxation can be neglected compared to translational relaxation. The additional oscillations described by Eq. (10) are called quantum beats (QB's) and originate from the coherent superposition of wave packets with slightly different energies. Figure 5 shows two original spectra in the limiting cases of large and small effective thickness of the sample. In order to avoid additional parameters in the fit procedure and to increase the statistics at the end of our time window, we integrated the time spectra over the QB oscillations. The in-

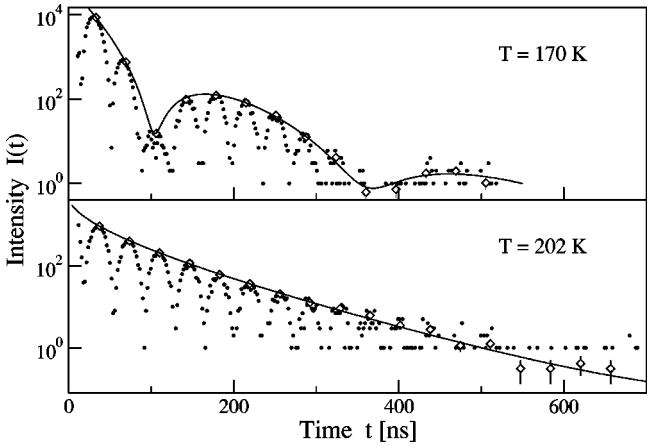

FIG. 5. Data treatment procedure: dots: original experimental data; diamonds: modified data corrected to the average intensity for one dynamical beat; solid line: fit to the modified data.

tegration was performed for each QB period, and the abscissae of the integrated data were set at the positions of the maxima of the beat pattern. The resulting set of points was fitted by Eq. (4), with modified incident intensity A'.

We checked the correctness of this procedure in the low-temperature region where relaxation is absent. Comparison of the fit parameters for original and integrated data shows agreement within the limit of the experimental error. Figure 5 shows this comparison between the original and the modified data for two temperatures. One can see that for $T = 202$ K the modified data is more informative in the time region after several τ_0 than the original one.

V. RESULTS

Figure 6 shows the delayed intensity emerging from the sample treated as pointed out in the previous section at various temperatures, starting from 173 K (below the calorimetric glass-transition temperature of 178 K) up to 202 K. All experimental data were fitted using Eqs. (4) and (10). For temperatures below 190 K additional fits have been performed with β fixed to 0.5 and 1 (Debye relaxation). The results for β (treated as a free parameter) are listed in Table I. Obviously β is quite stable and in average equal to 0.47 ± 0.02. In order to demonstrate the sensitivity of the experiment to changes of β, Fig. 7 shows fits of the spectra taken at 202 K with β fixed at 1, 0.75 and as free parameter.

In the low-temperature region, the large effective thickness (large Lamb-Mössbauer factor) leads to significant multiple scattering resulting in dynamical beats. Thanks to the nontrivial behavior of the dynamical beating, values for f_{LM} and τ_r can be determined with high accuracy since the cross correlation of the fit parameters is weak. As pointed out in the theoretical part of this paper, the shift of the minima of the dynamic beat oscillations in the case of a stretched relaxation allows to determine the stretching parameter β. One can see this effect comparing the exponential and the Kohlrausch fit of the data for example in Fig. 6 at $T = 188$ K. There is a small but clearly visible shift. Unfortunately the statistics of the data (as this concerns a minimum in intensity) is not very good. Nevertheless the fit gives a rather stable value of β in the entire temperature range.

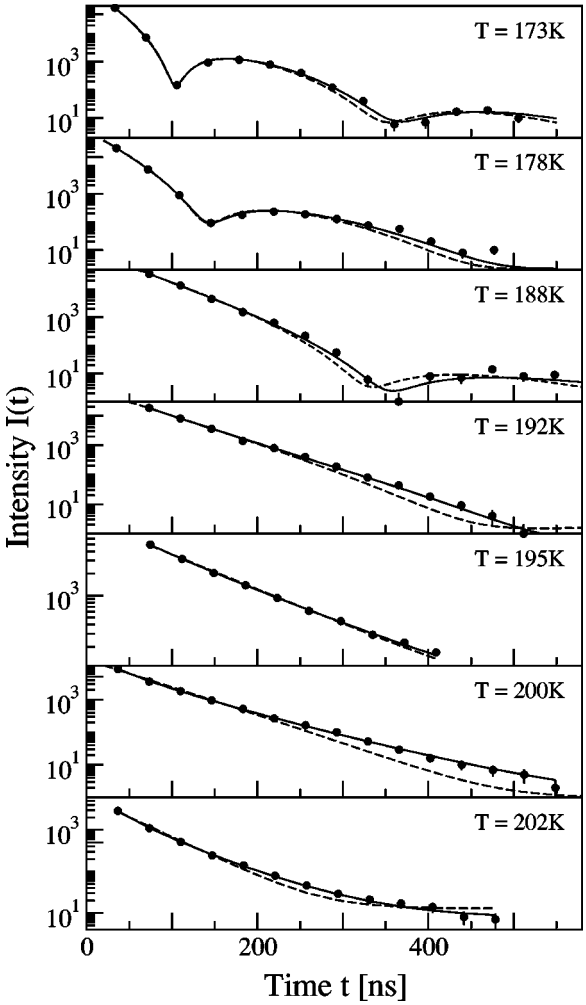

FIG. 6. Experimental data treated as pointed out in Sec. IV for selected temperatures. Solid line: fit as described in the text, dashed line: fit with β fixed to 1. In the last case the bending up of the fit curve is due to an unreasonably high background.

In the high-temperature region τ_r is small enough to see a clear bending-up in the data like in the theoretical picture (Fig. 1). At the same time f_{LM} is so small that the role of multiple scattering is weak. In this case multiple scattering manifests itself as an additional term in the exponent[27,16] as discussed at the end of Sec. II A, which reduces the apparent life time of the excited state. This fact prevents a unique separation of τ_r and f_{LM}. In order to resolve this problem, one has to use additional information. There are two ways to obtain this information: either the incoherent intensity is measured simultaneously by a second detector setup at a finite scattering angle[16] or the delayed rocking curve of the

TABLE I. Value of β for different temperatures.

T/K	173	178	188	192	195	200	202
β	0.46(15)	0.38(15)	0.48(15)	0.46(2)	0.49(1)	0.45(2)	0.48(2)

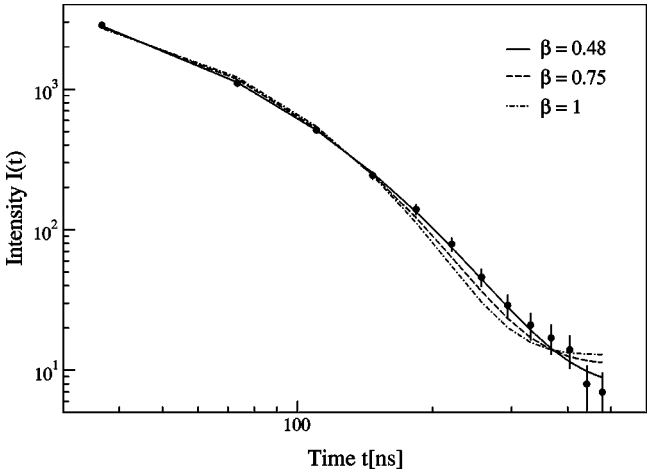

FIG. 7. Log-log picture of the intensity for $T=202$ K. Solid line: fit with β as a free parameter, dashed line: fit with β fixed to 0.75, dash-dotted line: fit with β fixed to 1.

high resolution monochromator is determined for each temperature.[30] We used both methods in our measurements and with this additional information we could determine τ_r and f_{LM} independently. Moreover, due to the large bending of the experimental curve we are able to get information about the stretching parameter β with rather high accuracy.

In Fig. 8 we show the temperature dependence of f_{LM} as obtained from the fits. The curve shows two distinct regions: at low temperatures a harmonic decrease and above $T \sim 150$ K a faster decay due to an additional process. We identify this process with the MCT β-relaxation,[11] a local rattling of the molecules in the cage formed by their neighbors.

In order to explain the harmonic part of the curve we used the high-temperature approximation of the Debye model for temperatures below 150 K. This yields a Debye temperature $\Theta=41$ K. For higher temperatures we added a square-root

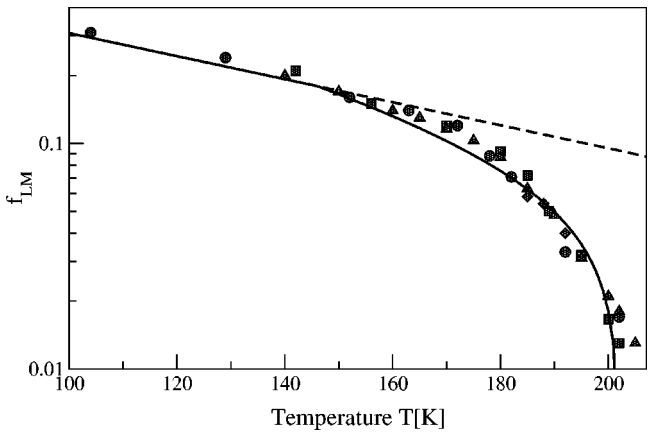

FIG. 8. Dependence of the Lamb-Mössbauer factor f_{LM} on temperature. The different symbols refer to different beam times. The solid line is a fit using the Debye model with $\Theta=41$ K below $T=150$ K. Above a square-root term $f_{\mathrm{LM}} \sim \sqrt{[(T_c-T)/T_c]}$ was added to the regular solution. The straight dashed line extends the low temperature data not shown in this figure.

behavior to the harmonic decay according to the MCT relation $f_q \sim \sqrt{(T_c-T)/T_c}$.[36] The solid line in Fig. 8 gives a value for the MCT crossover temperature T_c of 202(2) K. As expected for the high momentum transfer of NRS on ^{57}Fe, the nonergodicity parameter above T_c (named also critical form factor) is very small and below our detection limit.

VI. CONCLUSION

Our data allow to determine the relaxation parameters of a glass-forming liquid near and below the MCT crossover temperature T_c on atomic length scale. Using the Kohlrausch function to describe the α-relaxation we determined a stretching parameter $\beta=0.47(2)$. As NFS observes the relaxation at rather large wave vectors, the value of β determined in this experiment should be a good approximation for the von Schweidler exponent b describing the power law of the full MCT relaxation function.[36] Evaluating the square-root behavior of the nonergodicity parameter below T_c we found a critical temperature T_c of 202 K.

Those values may be compared to results of optical measurements performed on pure dibutyl phthalate.[37] In this work a T_c of 227 K and an exponent of $b=0.57$ was found. In comparing these values it must be noted, however, that in Ref. 37 the orientational relaxation is observed. It is well known that different correlators may lead to different relaxation times. In particular a decoupling of the translational from the orientational dynamics has been observed.[38]

The present result for β compares well with results obtained by numerical simulations of a Lennard-Jones system.[39] On the other hand glycerol, which is assumed to be a model system for medium strong glasses, has a stretching parameter of 0.7 (Ref. 40) which shows the range of possible values of this exponent.

The results for the relaxation time τ_r are identical to our earlier results[16] within the error bars. First indications of a relaxation on the time scale of microseconds appear already at 170 K even below the calorimetric glass-transition temperature. It should be noted that also Ruby *et al.*[35] have observed the onset of a line broadening effect at 175 K by conventional Mössbauer spectroscopy. Whereas the idealized MCT predicts a complete freezing of the system below T_c there are always thermally activated processes restoring ergodicity at long (macroscopic) times. This is included in the extended MCT by the so-called hopping parameter δ.[41] Above 190 K there is a steep increase in relaxation rate. For a more detailed discussion of the temperature dependence we refer to Ref. 16.

We would like to point out two important facts: On the one hand, in the kinematical approximation a large time window is required to see the stretched-exponential behavior of the self-correlation function near T_c. Therefore the extended time window as compared to our earlier experiment[16] is of crucial importance for the reliability of the data analysis. On the other hand, the analytical expression for the dynamical beat structure in the presence of arbitrary relaxation is mandatory to understand the effects seen in the temperature region where the kinematical approximation breaks down. It allows in principle to extract relaxation rates and β values

with high precision. Unfortunately the most significant effects appear at late times where the scattering intensity is low and accordingly the statistics is poor.

A drawback of the method used is that one cannot study any material but needs to insert dopant molecules containing a resonant nucleus. This is especially difficult in the case of the study of molecular glass formers, where small amounts of admixture may lead to crystallization. But this drawback converts to an advantage in the case where we study the behavior of a certain material as a function of the environment such as restricted geometry.[30] In this case the fact that we obtain a signal only from our sample not blurred by a signal from the environment improves the precision of such experiments or even makes them feasible. Also in this case, measurements using a long time window can be very interesting.[42] Information about changes in the shape of the relaxation modes due to a change of the environment will be the next step after the determination of the characteristic relaxation time in this case.

ACKNOWLEDGMENTS

The help of K. Messel and A. Ehnes, Hasylab, and A.I. Chumakov and O. Leupold, ESRF, during the experiments is appreciated. This work was supported by the German BMBF under Contracts No. 05 SK8 WOB 5 and KS1 WOC/2.

APPENDIX

After inserting $\varphi(\omega)$ from Eq. (3) into the expression for $E(\tau)$ from Eq. (2) and expanding the exponential in a power series we obtain

$$E(\tau)=\frac{A}{\tau_0}\delta(\tau)-\frac{A}{\tau_0}E_{\mathrm{del}}(\tau), \tag{A1}$$

$$E_{\mathrm{del}}(\tau)=\frac{A}{\tau_0}\xi_0 e^{-\tau/2}\sum_{k=0}^{\infty}(-1)^k\frac{\xi_0^k}{(k+1)!}\varphi^{(k)}(\tau), \tag{A2}$$

where $\varphi^{(k)}(\tau)$ is defined by the following recurrent expression:

$$\varphi^{(0)}(\tau)=F_s(\tau),$$

$$\varphi^{(k+1)}(\tau)=\int_0^{\tau}\mathrm{d}\tilde{\tau}\varphi^{(k)}(\tau-\tilde{\tau})F_s(\tilde{\tau}). \tag{A3}$$

It is more convenient to rewrite Eqs. (A2),(A3) in the following way:

$$E_{\mathrm{del}}(\tau)=\frac{A}{\tau_0}\xi_0 e^{-\tau/2}F_s(\tau)R(\tau), \tag{A4}$$

$$R(\tau)=\sum_{k=0}^{\infty}(-1)^k\frac{(\xi_0\tau)^k}{k!(k+1)!}\chi^{(k)}(\tau), \tag{A5}$$

where

$$\chi^{(0)}(\tau)=1,$$

$$\chi^{(k+1)}(\tau)=(k+1)\int_0^1 dx\,x^k\chi^{(k)}(x\tau)\frac{F_s[\tau(1-x)]F_s(\tau x)}{F_s(\tau)}. \tag{A6}$$

As a result the intensity of the delayed signal that is observed in NFS experiments can be written as

$$I(\tau)=I_{\mathrm{kin}}(\tau)R^2(\tau), \tag{A7}$$

$$I_{\mathrm{kin}}(\tau)=\left(\frac{A}{\tau_0}\right)^2\xi_0^2 e^{-\tau}F_s^2(\tau). \tag{A8}$$

Without diffusion $R(\tau)$ can be presented as

$$R(\tau)=\frac{J_1(2\sqrt{\xi\tau})}{\sqrt{\xi\tau}}. \tag{A9}$$

We denote with τ_i the position of the ith minimum point in the case without diffusion, $\Delta\tau_i$ is the shift of this point due to the relaxation described by the Kohlrausch self-correlation function. First we consider $\Delta\tau_i$ as a function of relaxation time when τ_r is much larger than 1. Then if we neglect fast relaxations that change only the effective thickness $F_s(\tau)\approx 1-(\tau/\tau_r)^{\beta}$. In this approximation Eq. (A6) converts to

$$\chi^{(k)}(\tau)\simeq 1-(\tau/\tau_r)^{\beta}Q_k(\beta), \tag{A10}$$

where $Q_k(\beta)$ is a rational positive function for any k and $Q_0(\beta)=0$. Using those definitions we may write

$$\begin{aligned}R(\tau)&=\sum_{k=0}^{\infty}(-1)^k\frac{(\xi\tau)^k}{k!(k+1)!}[1-(\tau/\tau_r)^{\beta}Q_k(\beta)]\\&=\sum_{k=0}^{\infty}(-1)^k\frac{(\xi\tau)^k}{k!(k+1)!}-(\tau/\tau_r)^{\beta}\\&\quad\times\sum_{k=0}^{\infty}(-1)^k\frac{(\xi\tau)^k}{k!(k+1)!}Q_k(\beta)\\&=R_0(\tau)-P(\tau)/\tau_r^{\beta},\end{aligned} \tag{A11}$$

where $R_0(\tau)$ is taken from Eq. (A9) and $P(\tau)$ is a function that does not depend on τ_r. Now we have to solve the equation $R(\tau_i+\Delta\tau_i)=0$.

$$R_0(\tau_i+\Delta\tau_i)-P(\tau_i+\Delta\tau_i)/\tau_r^{\beta}=0,$$

$$R_0(\tau_i)+R_0'(\tau_i)\Delta\tau_i=P(\tau_i)/\tau_r^{\beta},$$

$$\Delta\tau_i=\frac{P(\tau_i)}{R_0'(\tau_i)\tau_r^{\beta}}. \tag{A12}$$

As a result we get

$$\Delta\tau_i\sim 1/\tau_r^{\beta}. \tag{A13}$$

[1] U. Bengtzelius, W. Götze, and A. Sjölander, J. Phys. C **17**, 5915 (1984).
[2] H.Z. Cummins, Gen Li, Y.H. Hwang, G.Q. Shen, W.M. Du, J. Hernandez, and N.J. Tao, Z. Phys. B: Condens. Matter **103**, 501 (1997).
[3] M. Fuchs, J. Non-Cryst. Solids **172/174**, 241 (1994).
[4] R. Kohlrausch, Ann. Phys. (Leipzig) **12**, 393 (1847).
[5] G. Williams and D.C. Watts, Trans. Faraday Soc. **66**, 80 (1970).
[6] S. Havriliak and S. Negami, Polymer **8**, 161 (1967).
[7] K.S. Cole and R.H. Cole, J. Chem. Phys. **9**, 341 (1941).
[8] D.W. Davidson and R.H. Cole, J. Chem. Phys. **19**, 1484 (1951).
[9] M.D. Donsker and S.R.S. Varadhan, Commun. Pure Appl. Math. **28**, 525 (1975).
[10] G. Williams, M. Cook, and P.J. Hains, J. Chem. Soc., Faraday Trans. **68**, 1045 (1972).
[11] W. Götze and L. Sjögren, Rep. Prog. Phys. **55**, 241 (1992).
[12] J.B. Hastings, D.P. Siddons, U. van Bürck, R. Hollatz, and U. Bergmann, Phys. Rev. Lett. **66**, 770 (1991).
[13] G.U. Nienhaus and F. Parak, Hyperfine Interact. **90**, 243 (1994).
[14] A. Gahl, M. Hillberg, F.J. Litterst, T. Pöhlmann, C. Hübsch, O. Nuyken, F. Garwe, M. Beiner, and E. Donth, J. Phys.: Condens. Matter **10**, 961 (1998).
[15] G.V. Smirnov and V.G. Kohn, Phys. Rev. B **52**, 3356 (1995).
[16] A. Meyer, H. Franz, J. Wuttke, W. Petry, N. Wiele, R. Rüffer, and C. Hübsch, Z. Phys. B: Condens. Matter **103**, 479 (1997).
[17] M. Bée, *Quasielastic Neutron Scattering* (Adam Hilger, Bristol, 1988).
[18] J. Colmenero, A. Arbe, A. Alegria, M. Monkenbusch, and D. Richter, J. Phys.: Condens. Matter **11**, A363 (1999).
[19] K.S. Singwi and A. Sjölander, Phys. Rev. **119**, 863 (1960).
[20] K.S. Singwi and A. Sjölander, Phys. Rev. **120**, 1093 (1960).
[21] F. Mezei, *Neutron Spin Echo*, Lecture Notes in Physics No. 128 (Springer Verlag, Berlin, 1989).
[22] Hyperfine Interact. **123/124** (1999), edited by E. Gerdau and H. de Waard.
[23] V.G. Kohn and G.V. Smirnov, Phys. Rev. B **57**, 5788 (1998).
[24] Yu. Kagan, A.M. Afanas'ev, and V.G. Kohn, J. Phys. C **12**, 615 (1979).
[25] G.V. Smirnov, Hyperfine Interact. **123/124**, 31 (1999).
[26] U. van Bürck, Hyperfine Interact. **123/124**, 483 (1999).
[27] U. van Bürck, D.P. Siddons, J.B. Hastings, U. Bergmann, and R. Hollatz, Phys. Rev. B **46**, 6207 (1992).
[28] Yu.V. Shvyd'ko, Phys. Rev. B **59**, 9132 (1999).
[29] V.G. Kohn and G.V. Smirnov, Hyperfine Interact. **123/124**, 327 (1999).
[30] T. Asthalter, I. Sergueev, H. Franz, R. Rüffer, W. Petry, K. Messel, P. Härter, and A. Huwe, Eur. Phys. J. B **22**, 301 (2001).
[31] H. Franz, B. Huckelmann, and J.R. Schneider, Hyperfine Interact. **126**, 397 (2000).
[32] Yu.V. Shvyd'ko, E. Gerdau, J. Jäschke, O. Leupold, M. Lucht, and H.D. Rüter, Phys. Rev. B **57**, 4968 (1998).
[33] R. Rüffer and A.I. Chumakov, Hyperfine Interact. **97/98**, 589 (1996).
[34] T. Asthalter, R. Rüffer, and W. Petry (unpublished).
[35] S.L. Ruby, B.J. Zabransky, and P.A. Flinn, J. Phys. (Paris) **6**, C6-745 (1976).
[36] W. Götze, J. Phys.: Condens. Matter **11**, A1 (1999).
[37] D.D. Brace, S.D. Gottke, H. Cang, and M.D. Fayer, J. Chem. Phys. **116**, 1598 (2001).
[38] F. Fujara, B. Geil, H. Sillescu, and G. Fleischer, Z. Phys. B: Condens. Matter **88**, 195 (1992).
[39] E. Rabani, J.D. Gezelter, and B.J. Berne, Phys. Rev. Lett. **82**, 3649 (1999).
[40] J. Wuttke, W. Petry, and S. Pouget, J. Chem. Phys. **105**, 5177 (1996).
[41] M. Fuchs, W. Götze, S. Hildebrand, and A. Latz, J. Phys.: Condens. Matter **4**, 7709 (1992).
[42] P. Scheidler, W. Kob, and K. Binder, Europhys. Lett. **52**, 277 (2000).